

Energy transfer in Tm,Ho:KYW crystal and diode-pumped microchip laser operation

Sergey Kurilchik,^{1,2,*} Natali Gusakova,¹ Maxim Demesh,¹ Anatol Yasukevich,¹ Viktor Kisel,¹ Anatoly Pavlyuk,³ and Nikolai Kuleshov¹

¹Center for Optical Materials and Technologies, Belarusian National Technical University, 65/17 Nezavisimosti Ave., Minsk 220013, Belarus

²Kazan (Volga region) Federal University, 18 Kremlevskaya Str., Kazan 420008, Russia

³Nikolaev Institute of Inorganic Chemistry, Siberian Branch of Russian Academy of Sciences, 3 Lavrentyev Ave., Novosibirsk 630090, Russia

*kurilchik.sv@gmail.com

Abstract: An investigation of Tm-Ho energy transfer in Tm(5at.%)Ho(0.4at.%)KYW single crystal by two independent techniques was performed. Based on fluorescence dynamics measurements, energy transfer parameters P_{71} and P_{28} for direct (Tm→Ho) and back (Ho→Tm) transfers, respectively, as well as equilibrium constant Θ were evaluated. The obtained results were supported by calculation of microscopic interaction parameters according to the Förster-Dexter theory for a dipole-dipole interaction. Diode-pumped continuous-wave operation of Tm,Ho:KYW microchip laser was demonstrated, for the first time to our knowledge. Maximum output power of 77 mW at 2070 nm was achieved at the fundamental TEM₀₀ mode.

©2016 Optical Society of America

OCIS codes: (140.3580) Lasers, solid-state; (260.2160) Energy transfer; (140.3948) Microcavity devices.

References and links

1. K. Scholle, S. Lamrini, P. Koopmann, and P. Fuhrberg, "2 μm laser sources and their possible applications," in *Frontiers in Guided Wave Optics and Optoelectronics*, B. Pal, ed. (Intech, 2010).
2. S. A. Payne, L. K. Smith, W. L. Kway, J. B. Tassano, and W. F. Krupke, "The mechanism of Tm→Ho energy transfer in LiYF₄," *J. Phys. Condens. Matter* **4**(44), 8525–8542 (1992).
3. M. E. Storm and W. W. Rohrbach, "Single-longitudinal-mode lasing of Ho:Tm:YAG at 2.091 μm," *Appl. Opt.* **28**(23), 4965–4967 (1989).
4. G. L. Bourdet and G. Lescoart, "Theoretical modeling and design of a Tm, Ho:YLiF₄ microchip laser," *Appl. Opt.* **38**(15), 3275–3281 (1999).
5. J. Izawa, H. Nakajima, H. Hara, and Y. Arimoto, "A tunable and longitudinal mode oscillation of a Tm,Ho:YLF microchip laser using an external etalon," *Opt. Commun.* **180**(1-3), 137–140 (2000).
6. G. L. Bourdet and R. A. Muller, "Tm,Ho:YLF microchip laser under Ti:sapphire and diode pumping," *Appl. Phys. B* **70**(3), 345–349 (2000).
7. B. Q. Yao, F. Chen, C. T. Wu, Q. Wang, G. Li, C. H. Zhang, Y. Z. Wang, and Y. L. Ju, "Diode-end-pumped Tm,Ho:YVO₄ Microchip Laser at Room Temperature," *Laser Phys.* **21**(4), 663–666 (2011).
8. R. L. Zhou, Y. L. Ju, C. T. Wu, Z. G. Wang, and Y. Z. Wang, "A single-longitudinal-mode CW 0.25 mm Tm,Ho:GdVO₄ microchip laser," *Laser Phys.* **20**, 1320 (2010).
9. B. Q. Yao, F. Chen, P. B. Meng, C. H. Zhang, and Y. Z. Wang, "Diode Pumped Operation of Tm,Ho:YAP Microchip Laser," *Laser Phys.* **21**(4), 674–676 (2011).
10. P. Loiko, J. M. Serres, X. Mateos, K. Yumashev, N. Kuleshov, V. Petrov, U. Griebner, M. Aguiló, and F. Díaz, "Microchip laser operation of Tm,Ho:KLu(WO₄)₂ crystal," *Opt. Express* **22**(23), 27976–27984 (2014).
11. A. A. Lagatsky, F. Fusari, S. V. Kurilchik, V. E. Kisel, A. S. Yasukevich, N. V. Kuleshov, A. A. Pavlyuk, C. T. A. Brown, and W. Sibbett, "Optical spectroscopy and efficient continuous-wave operation near 2 μm for a Tm,Ho:KYW laser crystal," *Appl. Phys. B* **97**(2), 321–326 (2009).
12. A. A. Lagatsky, F. Fusari, S. Calvez, S. V. Kurilchik, V. E. Kisel, N. V. Kuleshov, M. D. Dawson, C. T. Brown, and W. Sibbett, "Femtosecond pulse operation of a Tm,Ho-codoped crystalline laser near 2 microm," *Opt. Lett.* **35**(2), 172–174 (2010).
13. B. M. Walsh, N. P. Barnes, and B. Di Bartolo, "On the distribution of energy between the Tm ³F₄ and Ho ⁵I₇ manifolds in Tm-sensitized Ho luminescence," *J. Lumin.* **75**(2), 89–98 (1997).
14. B. M. Walsh, N. P. Barnes, and B. Di Bartolo, "The temperature dependence of energy transfer between the Tm ³F₄ and Ho ⁵I₇ manifolds of Tm-sensitized Ho luminescence in YAG and YLF," *J. Lumin.* **90**(1-2), 39–48 (2000).

15. N. P. Barnes, E. D. Filer, C. A. Morrison, and C. J. Lee, "Ho:Tm lasers. I. Theoretical." *IEEE J. Quantum Electron.* **32**(1), 92–103 (1996).
16. S. R. Bowman, M. J. Winings, R. C. Y. Auyeung, J. E. Tucker, S. K. Searles, and B. J. Feldman, "Laser and spectral properties of Cr: Tm, Ho:YAG at 2.1 μm ." *IEEE J. Quantum Electron.* **27**(9), 2142–2149 (1991).
17. R. R. Petrin, M. G. Jani, R. C. Powell, and M. Kokta, "Spectral dynamics of laser-pumped $\text{Y}_3\text{Al}_5\text{O}_{12}:\text{Tm},\text{Ho}$ lasers." *Opt. Mater.* **1**(2), 111–124 (1992).
18. D. L. Dexter, "A theory of sensitized luminescence in solids." *J. Chem. Phys.* **21**(5), 836 (1953).
19. J. R. Lakowicz, *Principles of Fluorescence Spectroscopy* (Kluwer Academic Press, 2006).
20. I. Z. Steinberg, "Long-range nonradiative transfer of electronic excitation energy in proteins and polypeptides." *Annu. Rev. Biochem.* **40**(1), 83–114 (1971).
21. S. Bigotta, A. Toncelli, M. Tonelli, E. Cavalli, and E. Bovero, "Spectroscopy and energy transfer parameters of Tm^{2+} - and Ho^{2+} -doped $\text{Ba}_2\text{NaNb}_5\text{O}_{15}$ single crystals." *Opt. Mater.* **30**(1), 129–131 (2007).
22. A. Toncelli, M. Tonelli, E. Zannoni, E. Cavalli, and S. Cialdi, "NIR luminescence and laser parameters of $\text{Ca}_3\text{Sc}_2\text{Ge}_3\text{O}_{12}$ garnet host crystals activated with Tm^{2+} and Ho^{2+} ." *J. Lumin.* **92**(3), 237–244 (2001).
23. A. Brenier, G. Boulon, C. Madej, C. Pédrini, and L. Lou, "Kinetics of transfer and back transfer in thulium-holmium-doped $\text{Gd}_3\text{Ga}_5\text{O}_{12}(\text{Ca}, \text{Zr})$ garnet." *J. Lumin.* **54**(5), 271–277 (1993).
24. M. S. Gaponenko, P. A. Loiko, N. V. Gusakova, K. V. Yumashev, N. V. Kuleshov, and A. A. Pavlyuk, "Thermal lensing and microchip laser performance of Ng-cut $\text{Tm}^{3+}:\text{KY}(\text{WO}_4)_2$ crystal." *Appl. Phys. B* **108**(3), 603–607 (2012).

1. Introduction

Tm-sensitized Ho materials are considered to be among the most attractive solutions for lasers operating at wavelength slightly above 2 μm particularly when compact cavity design is required [1]. Tm^{3+} ions possess strong absorption near 800 nm where commercially available AlGaAs laser diodes operate. Two-for-one quantum efficiency caused by cross-relaxation process in thulium, and subsequent non-radiative energy transfer to Ho^{3+} ions enable efficient population of holmium $^5\text{I}_7$ manifold [2]. When in addition microchip cavity design is implemented the final laser source looks particularly compact and attractive for applications. Laser generation in microchip configuration has been achieved earlier with several Tm,Ho-codoped crystals such as: YAG [3], YLF [4–6], YVO_4 [7], GdVO_4 [8], YAP [9] and KLuW [10]. It was shown that Tm,Ho materials can be successfully used for obtaining laser radiation on holmium transition in such compact laser design. Recently efficient continuous-wave [11] and femtosecond pulse [12] laser operation has been reported using Tm,Ho:KY(WO₄)₂ (Tm,Ho:KYW) crystal under Ti-sapphire laser pumping. These results showed KYW crystal as an attractive host material for 2 μm lasers. There a description of the crystal growth, structure, spectroscopic properties and first results of evaluation of energy transfer parameters were presented. However energy transfer processes were studied incompletely and laser operation under diode-pumping was not obtained. Thus in this paper an investigation of Tm-Ho energy transfer parameters in KYW crystal by two independent techniques was undertaken and, for the first time to our knowledge, continuous-wave laser operation using this crystal in a microchip cavity configuration under diode laser pumping was demonstrated.

2. Study of energy transfer by fluorescence dynamics measurement

The study of energy transfer processes in Tm(5%),Ho(0.4%):KYW single crystal was implemented with an approach earlier described by B.M. Walsh in application to Tm,Ho-codoped YAG and YLF crystals [13,14]. According to this approach energy transfer parameters could be easily evaluated by fitting experimental data on fluorescence dynamics from $^3\text{F}_4$ energy level of Tm^{3+} ions and from $^5\text{I}_7$ level of Ho^{3+} ions to the solutions of rate equations set describing rates of change of energy levels population. In spite the fact that this approach doesn't take into consideration up-conversion processes in the ions and can be used only at low excitation densities it was important to find the parameters earlier calculated for other Tm,Ho-codoped crystals to compare them and to understand place of KYW crystal among other host materials.

In our experiment OPO based on $\beta\text{-BaB}_2\text{O}_4$ crystal and pumped by the third harmonic of actively Q-switched Nd:YAG laser was used as an excitation source of Tm and Ho fluorescence. The pulses had duration of 20 ns and repetition rate of 10 Hz. The fluorescence was collected by wide-aperture objective on entrance slit of monochromator MDR-12. The

signal was detected by InGaAs photodetector and processed by a digital oscilloscope with 500 MHz bandwidth. To eliminate influence of reabsorption on fluorescence dynamics a small piece of the crystal was grinded to crystalline powder and diluted by liquid silicone forming homogeneous suspension which then was used as the sample. Pulsed radiation at 1670 nm was used to selectively excite Tm^{3+} ions to $^3\text{F}_4$ energy level, while the wavelength was changed to 1960 nm for excitation of Ho^{3+} ions to $^5\text{I}_7$ energy manifold. The fluorescence dynamics were measured separately for Tm^{3+} ions at 1860 nm and for Ho^{3+} ions at 2056 nm. All the measurements were carried out at room temperature. The energy level transitions corresponding to absorption and emission wavelengths used in the experiment are shown in Fig. 1.

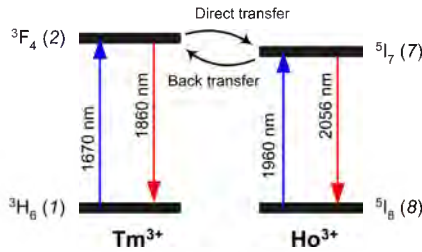


Fig. 1. Energy level transitions in Tm^{3+} and Ho^{3+} ions corresponding to absorption and fluorescence wavelengths used in the experiment.

The measured fluorescence dynamics of $\text{Tm}(5\text{at.}\%)\text{Ho}(0.4\text{at.}\%)\text{KYW}$ single crystal are shown in Fig. 2.

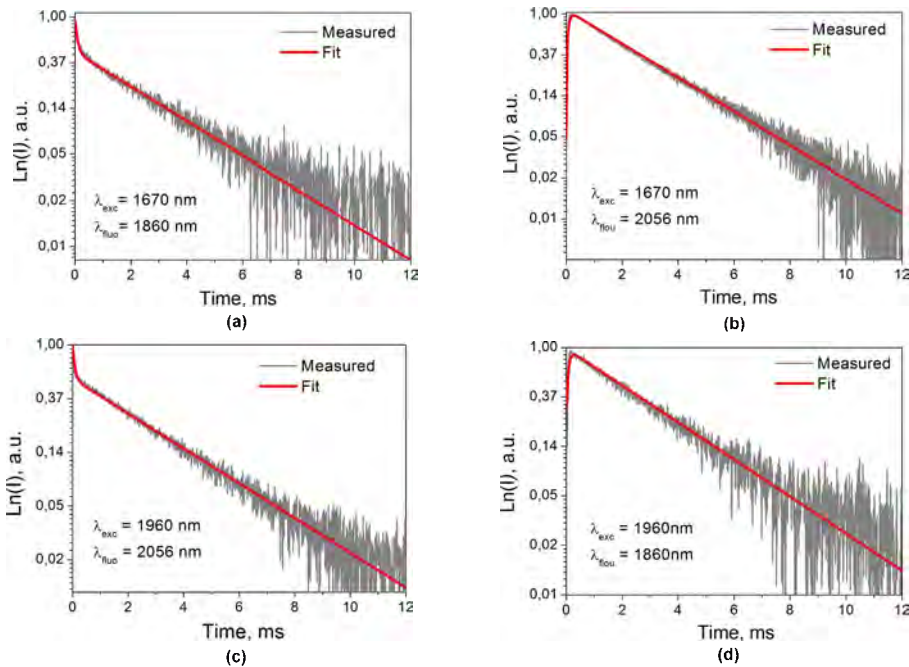


Fig. 2. Fluorescence dynamics of $\text{Tm}(5\text{at.}\%)\text{Ho}(0.4\text{at.}\%)\text{KY}(\text{WO}_4)_2$ crystal from $^3\text{F}_4$ manifold of Tm^{3+} ions (a) and from $^5\text{I}_7$ manifold of Ho^{3+} ions (b) under excitation of thulium at 1670 nm as well as from $^5\text{I}_7$ manifold of Ho^{3+} ions (c) and $^3\text{F}_4$ manifold of Tm^{3+} ions (d) under excitation of holmium at 1960 nm.

After Tm^{3+} ions excitation at 1670 nm fast decay of thulium fluorescence at 1860 nm is observed at early times (Fig. 2(a)) with simultaneous growth of fluorescence of holmium at

2056 nm (Fig. 2(b)). This behaviour results from direct energy transfer from Tm^{3+} to Ho^{3+} ions, where fast decrease of ${}^3\text{F}_4$ energy level population of Tm^{3+} accompanied by an increase of ${}^5\text{I}_7$ level population of Ho^{3+} . At later times fluorescence from both ions starts to decay exponentially with the same time constant, which was estimated to be 2.4 ms. This can be explained by the fact that growth of ${}^5\text{I}_7$ holmium population intensifies back energy transfer from Ho^{3+} to Tm^{3+} ions and quickly brings the ions to the state of thermodynamic equilibrium when populations of ${}^3\text{F}_4$ level of thulium and ${}^5\text{I}_7$ of holmium are determined by Boltzmann statistics as for a coupled system. It should be mentioned that this behavior is typical for Tm-Ho co-doped media [13]. Similar behaviour is observed when Ho^{3+} ions are excited at 1960 nm. Fast decay of holmium fluorescence at 2056 nm at early times (Fig. 2(c)) goes along with simultaneous growth of thulium fluorescence at 1860 nm (Fig. 2(d)), that is a consequence of back energy transfer from Ho^{3+} to Tm^{3+} ions. At later times fluorescence from both ions in similar manner exponentially decays with the same time constant, which in this case was estimated to be 2.7 ms. This behaviour denotes setting of thermodynamic equilibrium between ions.

The experimental curves were then fitted by the solutions of rate equations set governing the rate of change of populations in $\text{Tm}^{3+} {}^3\text{F}_4$ and $\text{Ho}^{3+} {}^5\text{I}_7$ manifolds [14] in case of thulium excitation:

$$\frac{n_2(t)}{n_2(0)} = \left(\frac{\beta}{\alpha + \beta} \right) \cdot \exp\left(-\frac{t}{\tau}\right) + \left(\frac{\alpha}{\alpha + \beta} \right) \cdot \exp(-(\alpha + \beta)t), \quad (1)$$

$$\frac{n_7(t)}{n_2(0)} = \left(\frac{\alpha}{\alpha + \beta} \right) \cdot \exp\left(-\frac{t}{\tau}\right) - \left(\frac{\alpha}{\alpha + \beta} \right) \cdot \exp(-(\alpha + \beta)t), \quad (2)$$

and in case of holmium excitation:

$$\frac{n_7(t)}{n_7(0)} = \left(\frac{\alpha}{\alpha + \beta} \right) \cdot \exp\left(-\frac{t}{\tau}\right) + \left(\frac{\beta}{\alpha + \beta} \right) \cdot \exp(-(\alpha + \beta)t), \quad (3)$$

$$\frac{n_2(t)}{n_2(0)} = \left(\frac{\beta}{\alpha + \beta} \right) \cdot \exp\left(-\frac{t}{\tau}\right) - \left(\frac{\beta}{\alpha + \beta} \right) \cdot \exp(-(\alpha + \beta)t). \quad (4)$$

Here the subscripts 1, 2, 7, and 8 denote the $\text{Tm} {}^3\text{H}_6$, $\text{Tm} {}^3\text{F}_4$, $\text{Ho} {}^5\text{I}_7$, and $\text{Ho} {}^5\text{I}_8$ manifolds, respectively (see Fig. 1). This indexing of the levels earlier was introduced by Barnes [15] and is used through this paper to get an agreement with the results obtained with other hosts. n_i is a population of i level, where $i = 2, 7$; τ is the time constant of exponential decay, α, β are the parameters determining direct and back energy transfer, respectively, which intrinsically are energy transfer probabilities with units of s^{-1} . These parameters are concentration dependent. However if they are divided to concentration of corresponding ions the obtained values will be energy transfer parameters [13]: $P_{28} = \alpha/N_{\text{Ho}}$ and $P_{71} = \beta/N_{\text{Tm}}$, which are concentration independent and characterize host material itself. N_{Ho} and N_{Tm} are the holmium and the thulium concentrations. P_{28} and P_{71} are the energy transfer parameters for direct and back energy transfer, respectively, with units of cm^3/s .

The best fitting for all experimental data both in case of thulium and holmium excitation was obtained with the same values of energy transfer probabilities: $\alpha = 7000 \text{ s}^{-1}$ and $\beta = 6100 \text{ s}^{-1}$. The energy transfer parameters P_{28} and P_{71} were calculated to be $2.74 \times 10^{-16} \text{ cm}^3/\text{s}$ and $0.19 \times 10^{-16} \text{ cm}^3/\text{s}$, respectively. We also found the ratio P_{71}/P_{28} , called equilibrium constant Θ [13]. In our case this value was estimated to be 0.069. The obtained results were tabulated in Table 1 in comparison with the data reported for other Tm,Ho-codoped laser crystals.

Table 1. Energy transfer parameters in Tm,Ho-codoped KYW crystal compared to other host materials at room temperature

Crystal	$\frac{P_{28} \times 10^{-16} \text{ cm}^3/\text{s}}{\times 10^{-16} \text{ cm}^3/\text{sec}}$	$\frac{P_{71} \times 10^{-16} \text{ cm}^3/\text{s}}{\times 10^{-16} \text{ cm}^3/\text{sec}}$	$\Theta = P_{71}/P_{28}$	Ref.
---------	--	--	--------------------------	------

Tm,Ho:KYW	2.74	0.19	0.069	[This work]
Tm,Ho:YAG	1.3	0.15	0.12	[14]
Tm,Ho:YAG	1.3	0.10	0.08	[16]
Tm,Ho:YAG	2.0	0.26	0.13	[17]
Tm,Ho:YLF	1.2-2.3	0.09-0.19	0.075	[14]

The Table 1 demonstrates that Tm,Ho:KYW crystal possesses the lowest equilibrium constant among other host materials with a significantly higher value of direct energy transfer parameter P_{28} . This shows KYW host material as a very promising candidate for Tm,Ho-codoping, which provides favourable conditions for direct energy transfer with regards to back transfer.

Assuming that all the excitation resides in the 3F_4 energy level of thulium and 5I_7 level of holmium we have also calculated a fraction of Ho^{3+} ion residing in the 5I_7 level at thermal equilibrium, $f_{Ho} = \alpha/(\alpha + \beta)$ [14]. The obtained value was to be 53.4%, which shows that more than a half of excitation energy in Tm(5at.%),Ho(0.4at.%):KYW crystal at low excitation densities transfers to Ho^{3+} ions. Additionally we found the value of f_{Ho} after increasing of holmium concentration up to 1 at. % with unchanged thulium concentration. The result was to be 74.2%. Further increase of holmium content up to 2 at.% leads to $f_{Ho} = 85.2\%$. So Tm,Ho:KYW crystals with higher doping level of holmium could be of interest for future investigation.

Fluorescence dynamics of Tm,Ho:KYW single crystal were also measured under excitation of thulium ions at 802 nm to higher lying 3H_4 energy manifold. The obtained results are shown in Fig. 3.

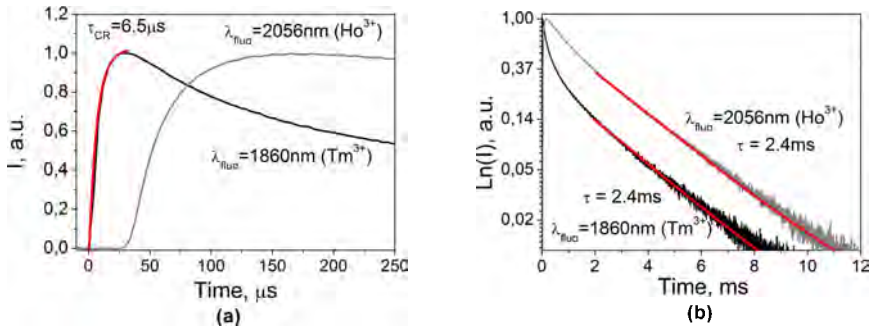


Fig. 3. Fluorescence dynamics of Tm and Ho ions in KYW single crystal under excitation of thulium at 802 nm at early times (a) and at later times (b).

Fast growth of thulium fluorescence notable at early times is attributed to cross-relaxation process in Tm^{3+} ions, leading to population of 3F_4 energy manifold. The time constant of this process was evaluated to be 6.5 μs . The further behavior of fluorescence is similar to the case of thulium 3F_4 excitation with setting of thermodynamic equilibrium at later times (Fig. 3(b)).

3. Energy transfer microparameters according to the Förster-Dexter theory

To support the results obtained from fluorescence dynamics measurement we calculated microscopic interaction parameters for our Tm,Ho:KYW single crystal according to Förster-Dexter theory of resonant energy transfer [18]. According to the theory microparameters of energy transfer from donor (D) to acceptor (A) ions $c_{D \rightarrow A}$ can be calculated with the expression:

$$c_{D \rightarrow A} = \frac{9c\chi^2}{16\pi^4 n^2} \int \sigma_D^{em}(\lambda) \sigma_A^{abs}(\lambda) d\lambda. \quad (5)$$

Here c is the velocity of light in vacuum, n – refractive index of the crystal, σ_D^{em} – emission cross-section of donor ion, σ_A^{abs} – absorption cross-section of acceptor ion, χ^2 is a factor describing the relative orientation in space of the transition dipoles of the donor and

acceptor. When the relative orientation of donors and acceptors in a medium is random, but fixed and do not change during excited state lifetime of the ions, as it is in case of crystalline matrix, the orientation factor χ^2 can be taken as 0.476 [19,20].

So the value of microparameter $c_{D \rightarrow A}$ according to Förster-Dexter theory is basically determined by the overlap of absorption and emission spectra of donor and acceptor ions. To calculate direct energy transfer microparameter $c_{Tm \rightarrow Ho}$, one must have emission spectrum of Tm^{3+} ions and absorption spectrum of Ho^{3+} ions in KYW crystal. Whereas to calculate back energy transfer microparameter $c_{Ho \rightarrow Tm}$, one must have emission spectrum of Ho^{3+} ions and absorption spectrum of Tm^{3+} ions in the crystal. The absorption spectra of the ions in KYW host were measured for singly doped crystals using spectrophotometer Cary 5000 at room temperature for polarization of light along principal axes N_m , N_p and N_g of the crystals. The emission cross-section spectra were calculated for each polarization by reciprocity method.

Polarization averaged absorption and emission cross-section spectra of Tm^{3+} and Ho^{3+} ions in KYW crystal are shown in Fig. 4.

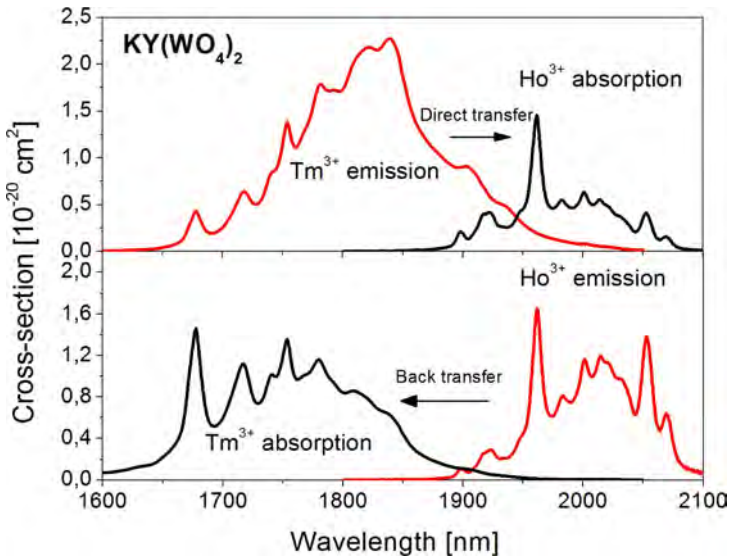


Fig. 4. Thulium emission and holmium absorption (upper) and holmium emission and thulium absorption (lower) cross-section spectra in KYW single crystal.

With Eq. (5) we calculated the values of interaction microparameters for direct and back energy transfers: $c_{Tm \rightarrow Ho} = 35.1 \times 10^{-40} \text{ cm}^6 \cdot \text{s}^{-1}$ and $c_{Ho \rightarrow Tm} = 2.16 \times 10^{-40} \text{ cm}^6 \cdot \text{s}^{-1}$, respectively. The energy transfer probabilities for a dipole-dipole interaction can be found by dividing microparameter to the six power of the distance between interacting ions. So the ratio $c_{Ho \rightarrow Tm}/c_{Tm \rightarrow Ho}$ will be equal to the ratio of energy transfer probabilities, which is analogous parameter to equilibrium constant Θ , that was calculated for this crystal from fluorescence dynamics measurements. After calculations $c_{Ho \rightarrow Tm}/c_{Tm \rightarrow Ho}$ was found to be 0.061. This value is in a good agreement with the value of equilibrium constant ($\Theta = 0.069$), that confirms the results of fluorescence dynamics analysis. The obtained results were tabulated in Table 2 in comparison with the data reported for other Tm, Ho-codoped hosts.

Table 2. Energy transfer microparameters in Tm, Ho-codoped KYW crystal according to Förster-Dexter analysis compared to other host materials

Crystal	$\frac{c_{Tm \rightarrow Ho}}{\times 10^{-40}}$	$\frac{c_{Ho \rightarrow Tm}}{\text{cm}^6 \cdot \text{sec}^{-1}}$	$\frac{c_{Ho \rightarrow Tm}}{c_{Tm \rightarrow Ho}}$	Ref.
Tm, Ho: KYW	35.1	2.16	0.061	[This work]
Tm, Ho: BNN	36.5	4.1	0.112	[21]
Tm, Ho: CaSGG	24	1.2	0.05	[22]

Tm,Ho:YAG	10.9	1.14	0.1049	[13]
Tm,Ho:YLF	16.9	1.24	0.0735	[13]
Tm,Ho:Gd ₃ Ga ₅ O ₁₂	10.5	0.3	0.0286	[23]

One can see from the table that the energy transfer coefficient $c_{\text{Tm} \rightarrow \text{Ho}}$ for Tm,Ho:KYW crystal is higher than that for the most of the other laser hosts. Also KYW shows a low value of the ratio $c_{\text{Ho} \rightarrow \text{Tm}}/c_{\text{Tm} \rightarrow \text{Ho}}$ that is lower than that observed in BNN (Ba₂NaNb₅O₁₅), YAG (Y₃Al₅O₁₂) and YLF (LiYF₄), and slightly higher than for CaSGG (Ca₃Sc₂Ge₃O₁₂) and Gd₃Ga₅O₁₂(Ca,Zr). However in these latter hosts, the value of the direct energy transfer process is much smaller than that of KYW.

4. Microchip laser experiment

To demonstrate a potential of Tm,Ho:KYW crystal for using in microchip laser devices we have carried out laser experiment with a laser diode (LD) as a pump source. Ng-cut Tm(5 at.%),Ho(0.4 at.%):KYW crystal with thickness of 2.98 mm was used as an active element. It was earlier shown that such orientation of the crystal is favorable for arising of positive thermal lens in the crystal that enables stability of plane-plane microchip cavity configuration [24]. The experimental setup of Tm,Ho:KYW laser is shown in Fig. 5.

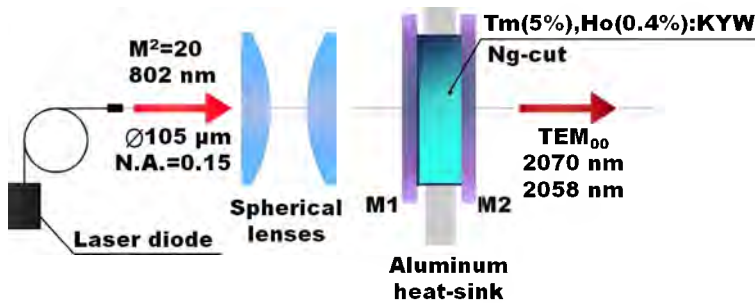


Fig. 5. Experimental setup of CW microchip laser.

Fiber-coupled ($\varnothing = 105 \mu\text{m}$, N.A. = 0.15) AlGaAs laser diode with maximum available output power of 3 W at 802 nm and $M^2 = 20$ was used as a pumping source. The diode wavelength was shifted to the absorption peak of the $^3\text{H}_4$ level (Tm³⁺) by temperature tuning of LD. The laser diode radiation was collimated and focused into the active element to a spot of 120 μm diameter with two spherical lenses ($f_1 = 70\text{mm}$, $f_2 = 80\text{mm}$). The laser resonator was formed by two plane mirrors which were positioned in close proximity to the ends of the active element. The HR plane input mirror M1 was AR coated for pump radiation (802 nm). Two output couplers with transmission of 0.8 and 1.8% were used. The crystal faces were AR-coated for the pump (802 nm) and laser (2.07 μm) radiations as well. The lateral sides of the laser crystal were in thermal contact with the aluminum heat sink whose temperature was precisely maintained with a thermoelectric cooler which temperature was to be 16°C.

CW laser operation was realized at the fundamental TEM₀₀ mode and lasing radiation was polarized along Np principal axis of the crystal. The laser performance characteristics are demonstrated in Fig. 6.

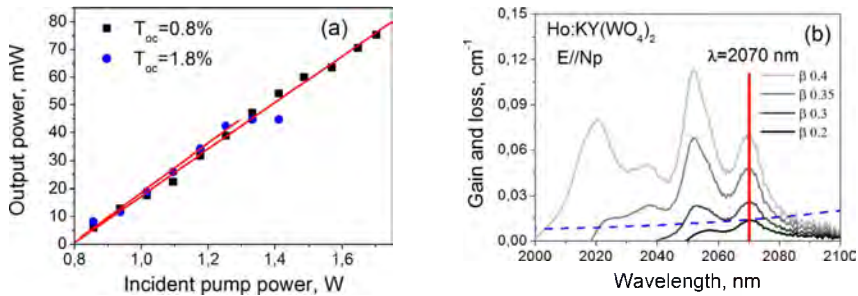


Fig. 6. Input-output characteristics of Tm,Ho:KYW laser (a) and gain spectra of Ho³⁺ ions in KYW (b).

The highest output power of 77 mW was obtained with 0.8% output coupler. The laser emission spectrum was centered at 2070 nm. This matches with a local maximum in the gain spectrum of Ho:KYW, see Fig. 6, dashed line represents losses ($T_{OC} = 0.8\%$). The corresponding slope efficiency of the laser with respect to incident pump power was estimated to be 8.5%. The laser threshold was about 0.8 W of incident pump power. The slope efficiency for output coupler $T_{OC} = 1.8\%$ at low pump power was higher than 9%, however maximum output power was limited by 46 mW. In the last case the laser wavelength shifted to 2058 nm that is attributed to higher level of cavity losses. Nonlinear dependence of the output power with respect to incident pump power and visible fluorescence was observed during lasing. Roll-over in input-output characteristic with higher output coupler transmission value (1.8%) was evident at 1.4 W of incident pump power. Such behavior can be caused by the higher up-conversion losses which increase heat release in the crystal. It's evident that higher transmission of the output coupler requires greater population inversion of the Ho³⁺ upper laser level ⁵I₇ and this leads to increase in up-conversion losses in the Tm, Ho:KYW. Similar behavior of Tm,Ho-laser was observed in [11].

5. Conclusion

Energy transfer in Tm(5at.%),Ho(0.4at.%):KYW single crystal has been investigated by two independent techniques. With an analysis of fluorescence dynamics of the crystal concentration independent energy transfer parameters for direct P_{71} and back transfer P_{28} processes were determined, which were $2.74 \times 10^{-16} \text{ cm}^3/\text{s}$ and $0.19 \times 10^{-16} \text{ cm}^3/\text{s}$, respectively. Equilibrium constant $\Theta = P_{28}/P_{71}$ was calculated to be 0.069. These results demonstrate domination of direct energy transfer in the crystal and in comparison with other host materials provides favourable conditions for population of ⁵I₇ energy level of holmium. A fraction of Ho³⁺ ions residing at ⁵I₇ energy manifold in the crystal at equilibrium constant was calculated to be 53.4%. An increase of this fraction was predicted with further growth of holmium content. The results obtained from fluorescence dynamics measurement were confirmed by independent calculation of interaction microparameters in accordance with Förster-Dexter theory. The microparameters were calculated to be $c_{Tm \rightarrow Ho} = 35.1 \times 10^{-40} \text{ cm}^6 \cdot \text{s}^{-1}$ and $c_{Ho \rightarrow Tm} = 2.16 \times 10^{-40} \text{ cm}^6 \cdot \text{s}^{-1}$. The ratio $c_{Ho \rightarrow Tm} / c_{Tm \rightarrow Ho}$ was to be 0.061, that is in a good agreement with the equilibrium constant obtained from fluorescence dynamics. CW laser operation with Tm,Ho:KYW in microchip configuration with LD pumping was realized for the first time to our knowledge. Maximum output power of 77 mW at 2070 nm was obtained with slope efficiency of 8.5% with respect to incident pump power. The laser was operating at the fundamental TEM₀₀ mode.

Acknowledgments

In a part of energy transfer this work was funded by the subsidy of the Russian Government (agreement No.02.A03.21.0002) to support the Program of Competitive Growth of Kazan Federal University among World's Leading Academic Centers. Microchip laser experiments were supported by Russian Science Foundation grant (Project # 15-12-10026).